



Tree Physiology 38, 264–276  
doi:10.1093/treephys/tpx124



## Research paper

# Why size matters: the interactive influences of tree diameter distribution and sap flow parameters on upscaled transpiration

Z. Carter Berry<sup>1,5</sup>, Nathaniel Looker<sup>2</sup>, Friso Holwerda<sup>3</sup>, León Rodrigo Gómez Aguilar<sup>4</sup>, Perla Ortiz Colin<sup>4</sup>, Teresa González Martínez<sup>3</sup> and Heidi Asbjornsen<sup>1</sup>

<sup>1</sup>Department of Natural Resources and the Environment, The University of New Hampshire, 46 College Road, Durham, NH 03824, USA; <sup>2</sup>Department of Soil Water and Climate, The University of Minnesota-Twin Cities, 1991 Upper Buford Circle, St Paul, MN 55108, USA; <sup>3</sup>Universidad Nacional Autónoma de México, Av. Universidad 3000, Ciudad de México D.F., 04510, Mexico; <sup>4</sup>Instituto de Ecología, Carretera antigua a Coatepec, Xalapa, Veracruz, 91070, Mexico; <sup>5</sup>Corresponding author (zcberry@gmail.com)

Received February 15, 2017; accepted September 13, 2017; published online October 13, 2017; handling Editor Nathan Phillips

In stands with a broad range of diameters, a small number of very large trees can disproportionately influence stand basal area and transpiration ( $E_t$ ). Sap flow-based  $E_t$  estimates may be particularly sensitive to large trees due to nonlinear relationships between tree-level water use ( $Q$ ) and tree diameter at breast height (DBH). Because  $Q$  is typically predicted on the basis of DBH and sap flow rates measured in a subset of trees and then summed to obtain  $E_t$ , we assessed the relative importance of DBH and sap flow variables (sap velocity,  $V_s$ , and sapwood depth,  $R_s$ ) in determining the magnitude of  $E_t$  and its dependence on large trees in a tropical montane forest ecosystem. Specifically, we developed a data-driven simulation framework to vary the relationship between DBH and  $V_s$  and stand DBH distribution and then calculate  $Q$ ,  $E_t$  and the proportion of  $E_t$  contributed by the largest tree in each stand. Our results demonstrate that variation in how  $R_s$  is determined in the largest trees can alter estimates up to 26% of  $E_t$  while variation in how  $V_s$  is determined can vary results by up to 132%. Taken together, these results highlight a great need to expand our understanding of water transport in large trees as this hinders our ability to predict water fluxes accurately from stand to catchment scales.

**Keywords:** sap flow, scaling, stand transpiration, tropical montane forests.

## Introduction

Sap flow techniques have been around for over 80 years (Huber 1932, Granier 1987, Burgess et al. 2001) and are the basis for some of the most frequently cited values of tree- and stand-level transpiration rates (e.g., Wullschlegel et al. 1998, Wilson et al. 2001). These methods are unique in their capacity to measure water use from the scale of tissues to whole plants at precise time intervals while logging over extended periods of time, fostering their use in addressing diverse questions across biological and hydrological sciences (e.g., Asbjornsen et al. 2011, Muñoz-Villiers et al. 2012, Berry et al. 2016). By allowing measurement and estimation (i.e., upscaling) of water fluxes across spatial and temporal scales, sap flow sensors provide a powerful tool for understanding how transpiration rates change in response to

environmental conditions, stand physiology (canopy-scale stomatal behavior) and structure (e.g., age, species and size distribution) across a variety of ecosystems (Schäfer et al. 2000, Köstner et al. 2002, Novick et al. 2009).

It has long been established that the procedure of upscaling sap flow measurements incorporates uncertainty at several points (Vertessy et al. 1997, Cermák et al. 2004, Jung et al. 2011). Generally, this uncertainty arises at two points, when applying velocity measurements to whole-tree water use and when using whole-tree water use to estimate landscape fluxes. A considerable body of work has assessed the former by considering how sap velocity, sapwood depth and wood properties (water content, basic density, thermal diffusivity, xylem wounding) vary within trees (e.g., Burgess et al. 2001, Ford et al.

2004, Alvarado-Barrientos et al. 2013, Looker et al. 2016). These studies have all drawn similar conclusions, that each of these traits can be scaled reliably to whole-tree water use with empirical functions. Unfortunately, a key knowledge gap still remains in assessing the uncertainty introduced when applying estimates of whole-tree water use to landscapes.

One notable study assessed landscape variation. Ford et al. (2007) found that upscaled stand level transpirations from sap flow were 14% lower than water balance calculations and that stand variation in sapwood area and basal area introduced most of this uncertainty. Generally, studies propose strategies to optimally allocate sampling efforts to constrain uncertainty in transpiration estimates (Ford et al. 2007, Kume et al. 2009). This includes, ideally, measurements of sap velocity and sapwood area (or depth) in trees that represent the entire range of species and size distributions in the area of interest (e.g., plot, stand or catchment; Köstner et al. 1998). Across trees within a site, tree-level water use ( $Q$ ) generally varies most directly in relation to size-related trends in leaf area and/or canopy position (Ryan and Yoder 1997, Čermák et al. 2004; but see Zimmermann et al. 2000); however, in common practice, researchers typically stratify sap flow sampling by selecting trees across a wide range of diameter (DBH, cm) classes (Oren et al. 1999). While great efforts are taken to stratify the sample, stands or landscapes are likely to include species and size classes outside of the sampled distribution. In the absence of alternative methods, measurements of  $Q$  in sampled trees are then used to develop an empirical function predicting  $Q$  on the basis of DBH in non-instrumented trees in the area of interest (Vertessy et al. 1997, Wullschlegel and King 2000, Meinzer et al. 2005, Mclannet et al. 2007, Cristiano et al. 2015). Stand level transpiration ( $E_t$ ,  $\text{I T}^{-1}$ ) can then be obtained by summing estimated  $Q$  across all the trees in an area and dividing by that area.

In addition to its applications for upscaling sap flow measurements, the relationship between water transport with tree size has received attention in many foundational studies (Ryan and Yoder 1997). While some researchers have proposed that physiological functioning increases as a quarter-power function of organism (tree) size (West et al. 1997, Enquist et al. 1998, Sperry et al. 2012, Smith et al. 2014), cross-site sap flow studies have indicated that, in some species, sigmoidal (or asymptotic) functions better approximate  $Q = f(\text{DBH})$  than do functions by which  $Q$  increases indefinitely with DBH (Jiménez et al. 1996, Meinzer et al. 2005, Kallarackal et al. 2013). Asymptotic relationships are further supported by known size-dependence of other biological exchange processes such as photosynthesis and respiration that diminish in larger trees (Yoder et al. 1994, Meir and Grace 2002, Mencuccini 2002, Niinemets 2002). The precise  $Q$ –DBH relationship will disproportionately affect predictions of water use in the largest trees.

Several studies conducted in a wide range of forest types have noted that a small number of large trees can transpire the

majority of water lost from a canopy (Köstner et al. 1992, Arneeth et al. 1996, Martin et al. 2000, Čermák et al. 2004). The disproportionate contribution of large trees to  $E_t$  may be driven by ecophysiological or stand phenomena, such as differences in water transport capacity (e.g., wood density, leaf and/or sapwood area), competitive ability for resources and/or crown microclimatic conditions across tree sizes (Barbour and Whitehead 2003, Fernández and Gyenge 2009, Mitchell et al. 2012, Kallarackal et al. 2013). Notwithstanding the plausibility of these biophysical explanations, the dependence of  $E_t$  on the water use of individual large trees may also be sensitive to (and possibly exaggerated by) assumptions about how  $Q$  increases with DBH; however, to our knowledge, this has not yet been systematically assessed.

In field studies,  $Q$  is not measured directly, but rather is estimated using DBH and measured sap flow parameters, namely sap velocity ( $V_s$ ) and sapwood area ( $A_s$ ) or sapwood depth ( $R_s$ ). The use of DBH as the scalar to derive  $Q$  introduces autocorrelation between those two variables (Oren et al. 1998, Meinzer et al. 2001). Hence, the form and parameters of the function  $Q = f(\text{DBH})$  result from the calculation of  $Q$  itself as well as the empirical relationships between DBH and measured sap flow parameters. The parameters  $V_s$ ,  $R_s$  and  $A_s$  have been shown to exhibit a wide range of possible relationships with DBH (Meinzer et al. 2001, Mclannet et al. 2007), as well as species (Link et al. 2014, Hernández-Santana et al. 2015, Looker et al. 2016), stand density (Benyon et al. 2015) and age (Zimmermann et al. 2000, Köstner et al. 2002). Additionally, climatic and phenological controls on the dynamics of leaf area and stomatal conductance cause  $V_s$  to vary from diurnal to interannual time scales (Jarvis 1976, Loustau et al. 1996, Mclannet et al. 2007). These factors collectively impart considerable variability in  $Q = f(\text{DBH})$  across sites and through time and may mediate the importance of large trees in determining  $E_t$ .

In this study, we examined how assumptions about the relationships between DBH and the sap flow parameters  $V_s$  and  $R_s$  affect estimates of tree- and stand-level transpiration ( $Q$  and  $E_t$ ) and the proportional contribution of large trees to  $E_t$ . We used stand structural data and measurements of  $V_s$  and  $R_s$  (82 trees, 10 species) from four tropical montane forest sites in central Veracruz, Mexico to develop a framework for modeling stand  $E_t$ . These data-driven simulations allowed us to determine how variation in the size-dependence of  $V_s$  and  $R_s$  alters  $Q$  and  $E_t$  across a range of stand structures. With this approach, we modeled distinct functions by which  $V_s$  and  $R_s$  could vary with DBH and applied these functions to simulate  $Q$  and  $E_t$  for simulated DBH distributions constrained by our observations. Due to the non-linear relationship between DBH and  $Q$ , we expected that  $E_t$  would increase with stand basal area and that the proportional contribution of the largest tree in each stand to  $E_t$  would be tightly related to the proportion of basal area associated with that same tree. Furthermore, we predicted that the magnitude of

$E_t$  and its dependence on the largest tree in the stand would be sensitive to the functional relationships between DBH and  $V_s$  and  $R_s$ . We tested these predictions in stands with contrasting DBH distributions and using DBH– $V_s$  relationships established during dry, wet and fog seasons over 2 years.

## Materials and methods

### Study region and description of sites

The study was conducted in tropical montane forests on the eastern slopes of Cofre de Perote volcano located in central Veracruz, Mexico (19°29'N, 97°02'W). All study sites were located at midslope elevations (1200–1500 m) and included three forests and one shade-coffee site. The climate is defined as 'temperate humid' by the Köppen classification modified by Garcia (1988). In the nearby city of Xalapa, the mean maximum annual temperature is  $27.1 \pm 1.5$  °C and mean annual rainfall is  $1463 \pm 231$  mm year<sup>-1</sup> (100-year record). This climate is highly seasonal with ~80% of rainfall occurring from June to October (henceforth 'wet season'). This wet season is followed by a cool, dry season from November to February characterized by milder temperatures and cold fronts that produce frequent fog events (henceforth 'fog season'). Finally, March–May is characterized by a warm, dry season as temperatures increase for several months before rain begins (henceforth 'dry season').

Soils of the site are Andisols with deep profiles, a silt-loamy texture and high organic matter content with high C/N ratios (Campos 2008). Additionally the soil horizons have high porosity (0.8 to  $-0.9$  cm<sup>3</sup> cm<sup>-3</sup>), low bulk density (0.2–0.8 g cm<sup>-3</sup>) and are generally considered nutrient-poor (Alvarado-Barrientos et al. 2014a, 2014b). Common tree species span diverse genera including *Carpinus*, *Liquidambar*, *Quercus*, *Platanus* and *Alchornea* (Williams-Linera 2002, Williams-Linera et al. 2013).

Forests of this region exist in a patchwork of disturbance regimes that come from historical clearing of lands for agricultural use, selective cutting for timber and natural turnover from tree mortality (Williams-Linera et al. 2002, Muñoz-Villers and López-Blanco 2008). Thus, to encompass this variation, we measured sap flow across secondary forests of three ages (~20 years, ~40 years and ~100 years) and one coffee agroforestry site. Canopy trees from the coffee site were included in this scaling analysis as they comprised all local montane forest species and exhibit similar diurnal patterns of water use as canopy trees from the forest sites. Within each site, eight representative trees across a wide diameter range were selected for sap flow measurements. In total, this included 82 trees ( $n = 39$  for sap velocity,  $n = 49$  for sapwood depth) of species ranging in DBH from 8 to 66 cm (see Table S1 available as Supplementary Data at *Tree Physiology* Online for tree details). The number of trees differed for each seasonal analysis because at one site not all trees were measured during all seasons. Measurements were conducted from January to July, 2014 for the ~100-year-old

forest site and from April to August, 2015 and January to March, 2016 for the remainder of the sites.

### Sap flow measurements and conversion to sap velocity ( $V_s$ )

Transpiration rates were determined using the heat ratio method (HRM) of sap flow (Burgess et al. 2001). This method has been regularly used in this region due to its ability to detect and quantify low and reverse flow rates that occur during fog events (Muñoz-Villers et al. 2012, Gotsch et al. 2014, Alvarado-Barrientos et al. 2013, 2014a, 2014b, Holwerda et al. 2016). The HRM utilizes three probes, installed perpendicular to the tree trunk, including a heater probe and two sensor probes spaced 0.6 cm in up- and downstream directions from the heater. Each sensor probe was equipped with three fine wire thermocouples spaced at radial depths of 0.5, 1.7 and 3 cm from the base of the probe. In a few smaller trees, only two thermocouples were utilized at depths of 1.1 and 2.2 cm. For some trees in the ~100-year-old forest the time to maximum temperature (T-max) method of Cohen et al. (1981) and modified by Kluitenberg and Ham (2004) was used, as the heat pulse velocities in these trees were higher than those that could be resolved with the HRM method (Holwerda et al. 2016). All sensors were constructed in the Asbjornsen Lab at the University of New Hampshire or in the Holwerda Lab at the Universidad Nacional Autónoma de México using identical construction protocols.

Prior to sensor installation, the bark was removed from the trunk at a height of ~1.3 m for probe insertion directly into the xylem. A metal drill bit guide (ICT International, Armidale, Australia) was mounted onto the exposed area to ensure accurate spacing and that drill holes were as perpendicular to the trunk face as possible. Once holes were drilled, probes were coated in petroleum jelly for conductivity and carefully inserted into the holes. Molding clay was placed around the sensor bases and reflective foam material was wrapped around the tree to avoid heating from direct sunlight. Ten meter extension cables from each sensor set ran to a central datalogging station consisting of a datalogger, multiplexer and an external 12 V battery (CR1000 and AM16/32; Campbell Scientific Inc., Logan, UT, USA). Every 15 min a heat pulse was sent to the heater probe and the change in temperature 60–100 s following the heat pulse of each thermocouple was recorded by the datalogger. In the ~100-year-old forest, raw temperature data were stored for subsequent calculations (Holwerda et al. 2016).

Using the methodology of Burgess et al. (2001), corrections for misalignment and wounding were conducted. Likewise, heat pulse velocities obtained with the T-max method were corrected for wounding following Cohen et al. (1981). For data sets from April to August, 2015, zero flow velocities were obtained by severing the sapwood immediately above and below the sensor sets. This method was consistent with zero flow calculations using the meteorological method to identify conditions likely to have zero or near-zero flow (e.g., Ambrose et al. 2010,

Gotsch et al. 2014). The corrected heat pulse velocities were converted to sap velocities ( $V_s$ ) using data on density and water content of the sapwood (Marshall 1958, Burgess et al. 2001). The latter were obtained from cores taken from trees located nearby the sample individuals. Small gaps in the data set (less than 3 h) were filled using an autoregressive integrated moving average (ARIMA) model. If days consisted of gaps larger than 3 h, the data were removed from the analysis. Prior to use in the scaling analysis,  $V_s$  rates measurements in individual trees were summarized as mean hourly rates across the radial sapwood fraction (average of the  $V_s$  values across three depths measured by our HRM sensors) during daytime hours (9:00–20:00 h local time). We summarized  $V_s$  in each tree separately for dry, wet and fog seasons.

### Sapwood depth measurement ( $R_s$ )

Sapwood depths were measured in 49 individuals spanning DBHs from 9.4 to 66 cm across five of the most common species of the region including *Carpinus tropicalis*, *Platanus mexicana*, *Clethra macrophylla*, *Quercus xalapensis* and *Quercus sartorii*. Because of challenges in clearly delineating sapwood boundaries in tropical regions, a range of methods and dyes were used to determine precise sapwood depths in each species. In *Q. xalapensis* and *Q. sartorii*, a 1% solution of bromocresol green in alcohol best presented the sapwood–heartwood boundary, while in *P. mexicana*, a 1% solution of hematoxylin was utilized. In each of these three species, a core was taken using an increment borer at breast height from each tree and brought to the lab for staining. The sapwood–heartwood boundary was carefully accessed under a stereoscope for each individual core. Two species, *C. macrophylla* and *C. tropicalis*, did not show clear delineations with staining in the laboratory and thus field techniques were used. Specifically, a 0.1% solution of indigo carmine was injected into a hole that had been drilled into a sample tree. The sample was left for 2 h with a slight pressure of 0.1 bar. Then a core was taken 4 cm above the injection point from which the sapwood depth could be clearly delineated (Meinzer et al. 2001). Finally, in each sample tree, DBH and depth of bark were also measured to more closely relate sapwood depth and DBH.

### Stand structure measurements

Stand structure data were collected by sampling all trees greater than 5 cm in 18 plots, 16 of which were 400 m<sup>2</sup> while an additional two were 113 m<sup>2</sup>. Plots spanned the greater tropical montane forest region and were all within an 8 km diameter circle. These additional two plots had different areas because they were pulled from an earlier study with a different sampling design. For each tree, the DBH, estimated height, crown diameter, species identity and GPS coordinates were collected. For individuals that were difficult to identify, branch samples were collected and taken back to the herbarium at the Instituto de Ecología (Xalapa, Mexico) for identification. Similar to sap flow measurements, plot data were collected across 18 forested sites

of various ages (six in mature forest, four in ~40 year old forest, four in ~20 year old forest and four in shade coffee forest) within the region to capture a representative set of size and species distributions within the region. Stand structure metrics obtained from different sized plots are presented on a per-hectare basis for standardization.

### Tree- and stand-level sap flow simulations

A simulation exercise was conducted to assess how the relationships between sap flow parameters ( $V_s$  and  $R_s$ ) and DBH affect tree- and stand-level transpiration rates ( $Q$ , l h<sup>-1</sup>), and  $E_t$ , mm h<sup>-1</sup>, respectively) across a range of DBH distributions. The exercise consisted of two sets of procedures: generation of DBH distributions within stands and simulation of sap flow parameters for each tree as a function of its DBH. For each of 1000 iterations, a 400-m<sup>2</sup> forest plot was simulated, in accordance with our stand structure sampling design. The number of individual trees in each plot ( $N$ ) was sampled from a uniform distribution from 5 to 85, resulting in a stand density that ranged from 125 to 2125 trees ha<sup>-1</sup>. We simulated the DBH distribution of each stand by drawing  $N$  samples from a three-parameter Weibull distribution (Bailey and Dell 1973, Aucoin 2015). Shape and location parameters of the Weibull distribution function were fixed to 1 and 5, respectively, so that simulated values fell within a realistic range of DBH. To approximate the density–diameter relationships observed in real forest stands (e.g., Zeide 1995), we imposed a negative relationship between the scale parameter of the distribution function and  $N$ , resulting in an inverse relationship between  $N$  and mean DBH and an asymptotic relationship between  $N$  and stand basal area (see Figures S1 and S2 available as Supplementary Data at *Tree Physiology Online*).

For each of the simulated DBH distributions, we tested the stand-level consequences of assumptions about how  $R_s$  and  $V_s$  vary with DBH. We simplified the representation of sap flow-related variables (e.g., by assuming a circular stem cross-sectional area and disregarding radial variation in  $V_s$ ) in order to evaluate how methodological decisions affect the magnitude of  $E_t$  and its dependence on a small number of large trees. To estimate sap flow ( $Q$ ) for each tree,  $R_s$  was predicted on the basis of DBH or as a proportion of the sapwood depth (described in more detail in the following paragraph). Then,  $V_s$  was multiplied by the cross-sectional ring corresponding to the radial fraction measured by the sensor (with sensor depth equal to 0.5, 1.7 and 3 cm, depending on  $R_s$ ). Next, assuming that  $V_s$  declined linearly from the tip of the sensor to the sapwood–heartwood boundary, the fraction of sapwood area beyond the tip of the sensor was multiplied by the value of  $V_s$  estimated for the point halfway between the tip of the sensor and  $R_s$ . The sum of the two products yields  $Q$ , which is equivalent to whole-tree transpiration under conditions of steady-state water use; the sum of  $Q$  for trees within a stand is taken as stand-level transpiration ( $E_t$ ). The estimates of  $E_t$  were then compared relative to two



theoretical values of evapotranspiration. First, we compared  $E_t$  to net radiation, which can be considered as the absolute maximum available energy for  $E_t$ . Secondly, transpiration in these humid tropical forests is typically 70–80% of net radiation and thus we used 80% of this value as another point of comparison (Holwerda et al. 2016). Net radiation was estimated from measured shortwave radiation and assuming a fixed albedo of 0.12. Furthermore, net longwave radiation was estimated by multiplying black body radiation at air temperature by a net emissivity factor (calculated from actual vapor pressure) and by a cloudiness factor (calculated from observed shortwave radiation and estimated clear-sky radiation) (Holwerda et al. 2016). While these estimates provide an approximation of potential water use, we acknowledge that there is no direct measure of evapotranspiration (e.g., eddy covariance).

Using these methods to calculate  $Q$  and  $E_t$  for each simulated stand, we conducted two complementary analyses, focusing separately on how  $E_t$  is affected by the relationships between DBH and  $R_s$  and  $V_s$ . First, we compared two approaches to

predicting  $R_s$  (and thus  $A_s$ ) on the basis of DBH. The first model assumed that  $R_s$  increased linearly with DBH (Figure 1A; Meinzer et al. 2001), whereas the second model assumed a linear relationship between DBH and  $R_s$  as a proportion of the trunk radius (sapwood fraction,  $P_s = R_s / (DBH/2)$ , Figure 1B). Both models were fit as quantile regressions (Koenker 2016), with the response variable ( $P_s$ ) defined as the median value at a particular DBH. Quantile regression was chosen over simple linear regression after we detected non-homogeneous variance in measured  $P_s$  across the DBH range (Figure 1B); this change in spread can be represented as an envelope of  $P_s$  values by including upper and lower quantiles (2.5th and 97.5th percentiles) in the model. After using these regressions to obtain median  $R_s$ ,  $A_s$  was calculated as the difference between tree basal area ( $\pi * (DBH/2)^2$ ) and heartwood area ( $\pi * (DBH/2 - R_s)^2$ ) (Figure 1C). Differences in  $E_t$  resulting from these two  $R_s$  scaling scenarios were assessed by first calculating  $Q$  for each simulated tree using the median value of  $V_s$  (i.e., ignoring DBH effects on  $V_s$ ), summing  $Q$  to obtain  $E_t$  and then subtracting the  $E_t$  value

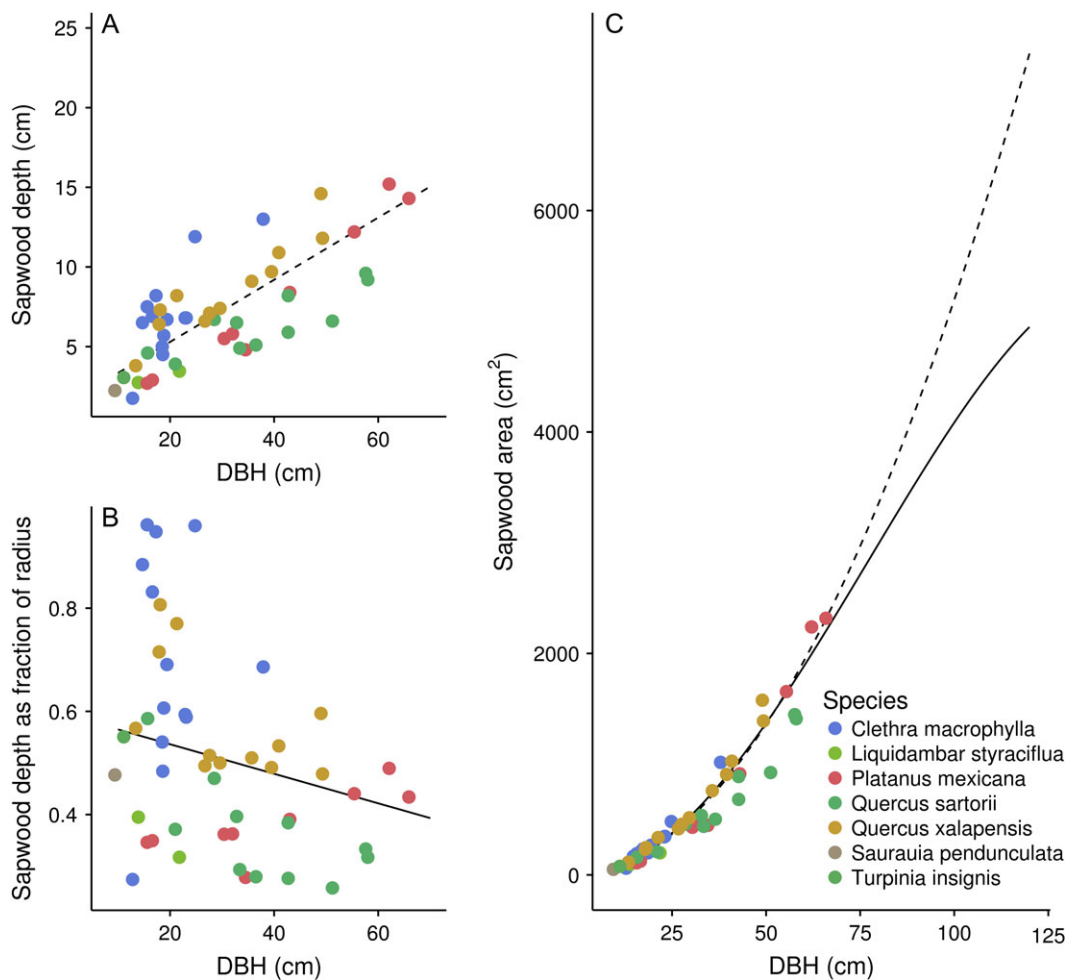


Figure 1. Relationship between sapwood depth and DBH (A) and sapwood depth as a fraction of the radius and DBH (B). Data points are derived from all trees in the study and lines represent best fit regressions. Panel (C) represents total sapwood area by DBH for all trees with dotted and solid lines representing the extrapolation from the best fit lines in (A) and (B).

from the scenario in which  $P_s$  scales linearly with DBH from the scenario in which  $R_s$  scales linearly with DBH. This difference was also expressed as a relative error by dividing by the  $E_t$  value from the  $P_s$  scenario (generally the more conservative value). We also calculated the difference in the proportion of  $E_t$  contributed by the largest tree within each stand for both scaling scenarios.

The second set of analyses addressed the scaling of  $V_s$  with DBH. Previous studies have noted a wide range of possible relationships between DBH and  $V_s$ , from null to either positive or negative (Meinzer et al. 2001, McInnet et al. 2007). We detected a positive relationship between DBH and mean hourly  $V_s$  across seasons (Figure 2), largely driven by species changes across the DBH range. Because we were concerned with stand-level patterns regardless of the underlying mechanisms (e.g., species, canopy position, etc.), we fit quantile regressions to predict median  $V_s$  for all trees during each season as a function of DBH (Figure 2, Table 1). Taking the case of linear scaling of  $V_s$  with DBH as an upper limit to  $Q$  and  $E_t$ , we considered a series of alternative scaling

scenarios in which  $V_s$  would remain constant above a particular value of DBH (successive 10 cm; horizontal lines in Figure 2). We included this piecewise scaling to quantify the possible errors in  $E_t$  (and its dependence on large trees) if the  $Q = f(\text{DBH})$  is established with the implicit assumption that  $V_s$  can increase indefinitely with tree size. As with the  $R_s$  scaling scenarios, we calculated the difference in  $E_t$  and the proportion of  $E_t$  contributed by the largest tree across all scenarios, normalizing the difference between the  $E_t$  values obtained from linear and piecewise scenarios relative to the piecewise scenario values. All simulations and analyses were conducted in R version 3.3.2 (R Development Core Team 2016).

## Results

### Characterizing relationships between DBH and sap flow parameters

To characterize the scaling relationships between tree diameter (DBH) and sap flow parameters, quantile regressions were

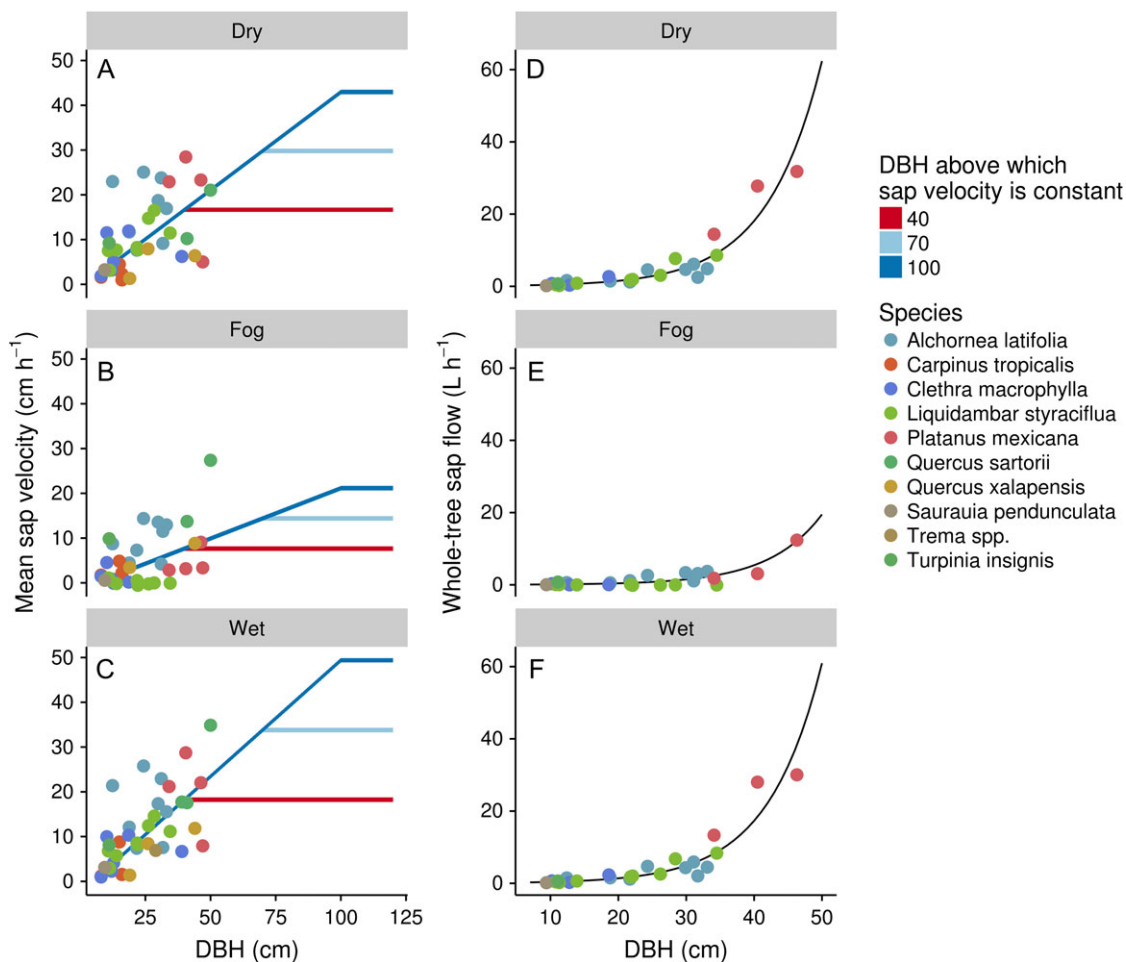


Figure 2. Mean sap velocity by DBH for all trees in the study from dry (A), fog (B) and wet (C) seasons. The initial solid line represents the best fit linear regression. Horizontal lines at subsequent points represent the range of possibilities examined within the subsequent modeling simulations. We assumed that  $V_s$  would not linearly increase forever and thus tested each of these points where values might asymptote. The specific colored lines (red, light blue, dark blue) represent asymptotes at 40, 70 and 100 cm DBH and correspond to the same colors used in Figure 4. Panels (D–F) represent the scaling to whole-tree  $Q$  assuming that the linear relationships to the left are true across all three seasons, which gives an exponential output.

Table 1. Quantile regression models predicting median value of sap flow parameters ( $P_s$ : sapwood depth as a fraction of tree radius;  $R_s$ : sapwood depth in cm;  $V_s$ : sap velocity in  $\text{cm h}^{-1}$ ) as a function of DBH. Regression coefficients were estimated using the quantreg package (version 5.29) in R (version 3.3.2), with standard errors approximated through a bootstrap procedure. These models were fit to data pooled across species and sites ( $n = 49$  trees for  $R_s$  and  $P_s$ ;  $n = 39, 35$  and  $37$  trees for  $V_s$  during wet, fog and dry seasons, respectively).

Model	Parameter	Value	Std error	t-value	P-value
Ps	(Intercept)	0.593	0.060	9.721	<0.001
Ps	DBH	-0.003	0.002	-1.481	0.145
Rs	(Intercept)	1.390	1.297	1.072	0.289
Rs	DBH	0.195	0.045	4.298	<0.001
Vs_wet	(Intercept)	-2.520	2.638	-0.955	0.346
Vs_wet	DBH	0.519	0.125	4.158	<0.001
Vs_dry	(Intercept)	-0.862	3.068	-0.281	0.781
Vs_dry	DBH	0.438	0.164	2.667	0.011
Vs_fog	(Intercept)	-1.326	1.592	-0.833	0.411
Vs_fog	DBH	0.225	0.104	2.163	0.038

performed between DBH and sapwood depth ( $R_s$ ), sapwood depth as a fraction of radius ( $P_s$ ) and sap velocity ( $V_s$ ; Figures 1 and 2, Table 1). There was a significant positive relationship between  $R_s$  and DBH after accounting for species-specific intercepts ( $P < 0.001$ ), highlighting that mean sapwood depth generally increased with increasing DBH within the range of sizes sampled (Table 1, Figure 1A). We also detected a negative relationship between DBH and  $P_s$  (Figure 1B). These two distinct approaches to modeling the relationship between DBH and sapwood depth (i.e.,  $R_s$  or  $P_s$  scales linearly with DBH) led to divergent estimations of total sapwood area for trees. When sapwood area was calculated with  $R_s$ , sapwood area scaled exponentially with DBH, whereas the use of  $P_s$  led to a sigmoidal relationship (Figure 1C). As with  $P_s$ ,  $V_s$  varied significantly with DBH only when species were pooled ( $P = 0.0018$  for slope coefficient in simple linear regression of dry-season  $V_s$  compared with  $P = 0.414$  for model with species-specific intercepts). These findings were consistent across all three seasons in the study region (Figure 2), with reduced sap velocities during the fog season leading to an apparent decrease in slope ( $0.426 \text{ cm h}^{-1} \text{ cm}^{-1}$  in the wet season,  $0.311 \text{ cm h}^{-1} \text{ cm}^{-1}$  in the dry season and  $0.249 \text{ cm h}^{-1} \text{ cm}^{-1}$  in the fog season), again explained by species differences.

### Characterizing plot diversity, size distributions and influence on stand transpiration

Eighteen plots were sampled for size and species distributions to assess variation in multiple variables across the plots (Figure 3). The number of stems in a plot ranged from just 5 trees to 117 trees and the DBH of the largest tree in a plot ranged from 29 to 109 cm. To determine the relative influence of tree diameters on stand structural metrics (namely, basal area) and total stand transpiration, the percentage contribution of each tree size class to stand-level estimates was derived. Most plots

were dominated by trees smaller than 30 cm DBH (Figure 3A–C). When comparing the distribution of tree diameters across increasing plot basal area, there was a general trend towards a greater number of larger single trees and fewer smaller trees (from A to C in Figure 3). The percentage of transpiration coming from each size class followed a less consistent pattern with the largest influences typically coming from medium or larger trees. The largest influence of one size class typically occurred above 40 cm DBH and often in trees above 70 cm DBH (Figure 3D–F). Equally important, the absolute value was often larger for the peak values with the most important size class typically predicting well over 50% of the plot transpiration from a single size class. These size distributions were used as a base for developing a set of plot distributions in the simulation exercises.

### Stand sap flow simulations

The scenarios concerning the scaling of sapwood depth with DBH yielded qualitatively different conclusions from the scenarios involving sap velocity. The two sapwood depth scenarios (i.e., with either  $R_s$  or  $P_s$  scaling linearly with DBH) resulted in estimates of  $E_t$  that diverged by up to  $0.1 \text{ mm h}^{-1}$ , or 26% of  $E_t$  as estimated in the DBH- $P_s$  scenario. For  $V_s$ , the difference between the two extreme scenarios ( $V_s$  scaling linearly with DBH versus remaining constant above 40 cm DBH) produced estimates of  $E_t$  that diverged up to  $0.78 \text{ mm h}^{-1}$ , or 132% of  $E_t$ . When plots had trees larger than 40 cm DBH, the slope of the relationship between stand transpiration and basal area was steeper across all three seasons (Figure 4, Table 1). Specifically, the stand transpiration estimates surpassed the constrained theoretical upper limits derived from the maximum available energy for  $E_t$  (Figure 4, solid and dotted horizontal lines). For stands with large trees, all estimates were greater than the maximum available energy when sap velocity was allowed to increase until 100 cm DBH. When sap velocity was held constant at lower DBHs (e.g., 40 cm), this maximum was reached only at high stand basal areas. For ease of demonstration, only simulations where sap flow was held constant above 40, 70 and 100 cm DBH are shown in Figure 4.

We further considered the influence of the largest tree to stand transpiration rates relative to stand basal area (Figure 5). When allowing  $V_s$  to vary based on the DBH where sap flow was held constant produced significant variation in the contribution of the largest tree to stand transpiration (Figure 5, left). Importantly, the majority of these values fell above the default 1:1 line meaning that the contribution of the largest tree to stand transpiration is greater than the contribution to basal area. When  $V_s$  was held constant and  $R_s$  allowed to vary, results were much more consistent and fell near the 1:1 line meaning that variation in  $R_s$  had less influence on the contribution of large trees to stand transpiration. Finally, a comparison of the stand level outputs when  $V_s$  or  $R_s$  were allowed to vary while the other was held

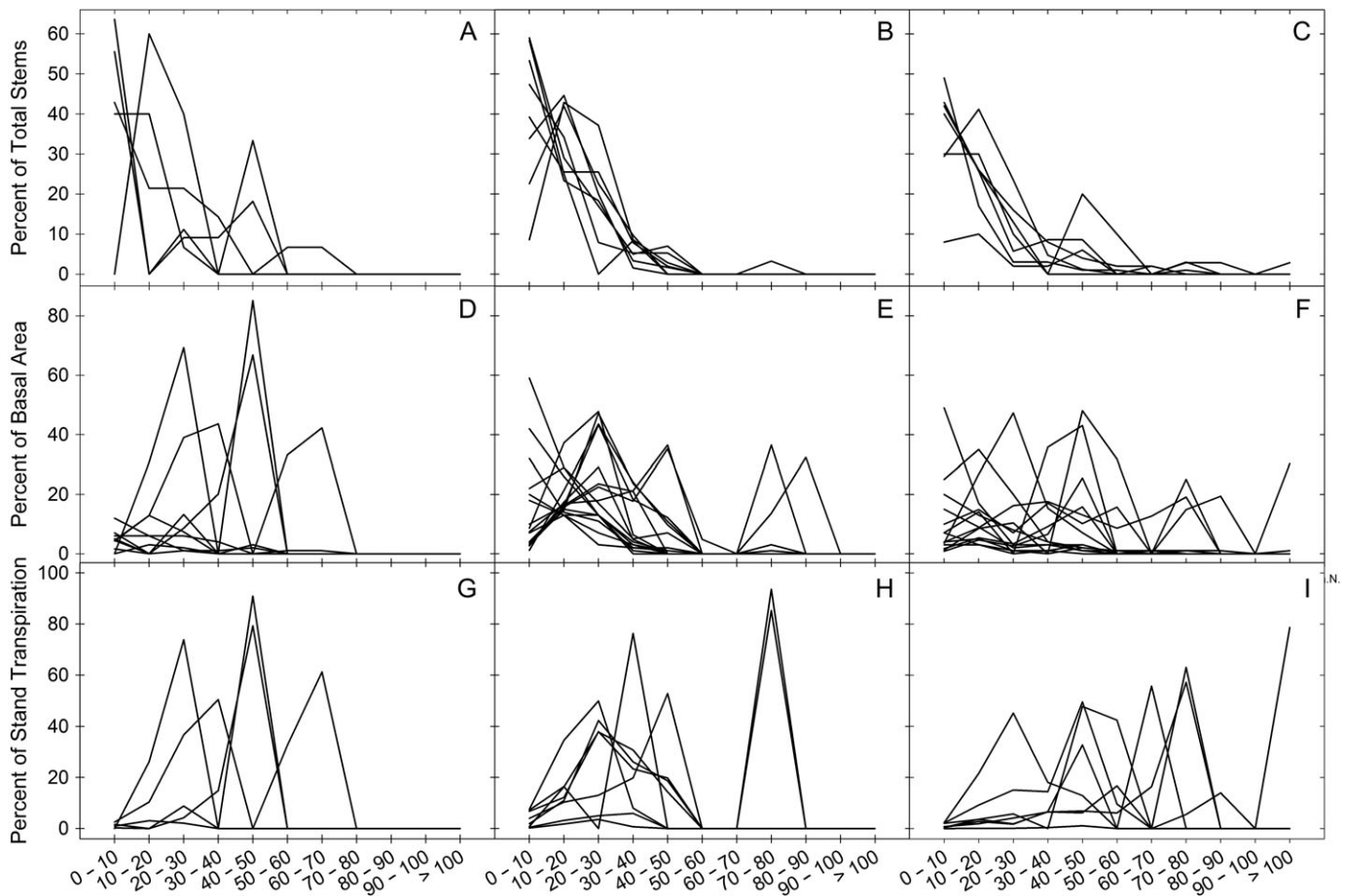


Figure 3. The percentage of stems (A–C), percentage of stand basal area (D–F) and percentage of stand transpiration (G–I) from each size class binned in 10 cm groups. Plots are separated into those with total stand basal areas below 20 m<sup>2</sup> ha<sup>-1</sup> (A, D and G), 20–40 m<sup>2</sup> ha<sup>-1</sup> (B, E and H) and greater than 40 m<sup>2</sup> ha<sup>-1</sup> (C, F and I). Generally transpiration skews disproportionately towards medium and larger size classes while the proportion of stems skews towards lower size classes.

constant produced high variation in their outputs depending on the DBH sap velocity that was held constant (Figure 6). As expected, the variation between the groups was reduced if the constant DBH was very high (e.g., 100 cm DBH).

## Discussion

Our results demonstrate that fundamental assumptions about the empirical relationships between sap flow scalar parameters and tree size can have a significant impact on tree- and stand-level estimates of water fluxes ( $Q$  and  $E_t$ , respectively). Modeling exercises exploring a broad range of stand structures (i.e., stem density and DBH distributional characteristics) revealed how the scaling of sap flow parameters (sapwood depth and sap velocity,  $R_s$  and  $V_s$ ) with DBH gives rise to distinct relationships between stand basal area and  $E_t$  (Figure 4). Importantly, this means that  $E_t$  cannot be accurately predicted on the basis of stand structure and basal area alone. At a given basal area, estimates of  $E_t$  diverged by up to 132% depending on how  $V_s$  was assumed to scale with DBH, while the  $R_s$  scenarios diverged by up to 26%.

In addition to these differences in  $E_t$ , our modeling results indicated that the largest trees in a plot can contribute the majority of  $E_t$  (e.g., 98% when the largest tree is 4.4 times greater than the median DBH and stem density is low) and that the magnitude of that contribution also depends on the scaling of sap flow parameters with DBH (Figures 5 and 6). Taken together, these findings underscore the need for more targeted characterization of sap flow parameters and quantification of water transport in large trees, which hinder predictions of landscape water fluxes.

Though we were unable to measure  $R_s$  and  $V_s$  in the largest trees in our study sites, we argue that the plausible envelope of these variables across the range of DBH can be constrained using available field data and by considering the physical limitations on water transport. At the stand level, we estimated a maximum value of potential  $E_t$  for each season if evapotranspiration were limited only by net radiation (i.e., zero hydraulic, stomatal, boundary layer resistances, and zero turbulent and storage fluxes of sensible heat). Estimates of  $E_t$  were greater than net radiation when  $V_s$  was held constant at 100 cm DBH. Additionally, when  $V_s$  was held constant at lower DBHs, this



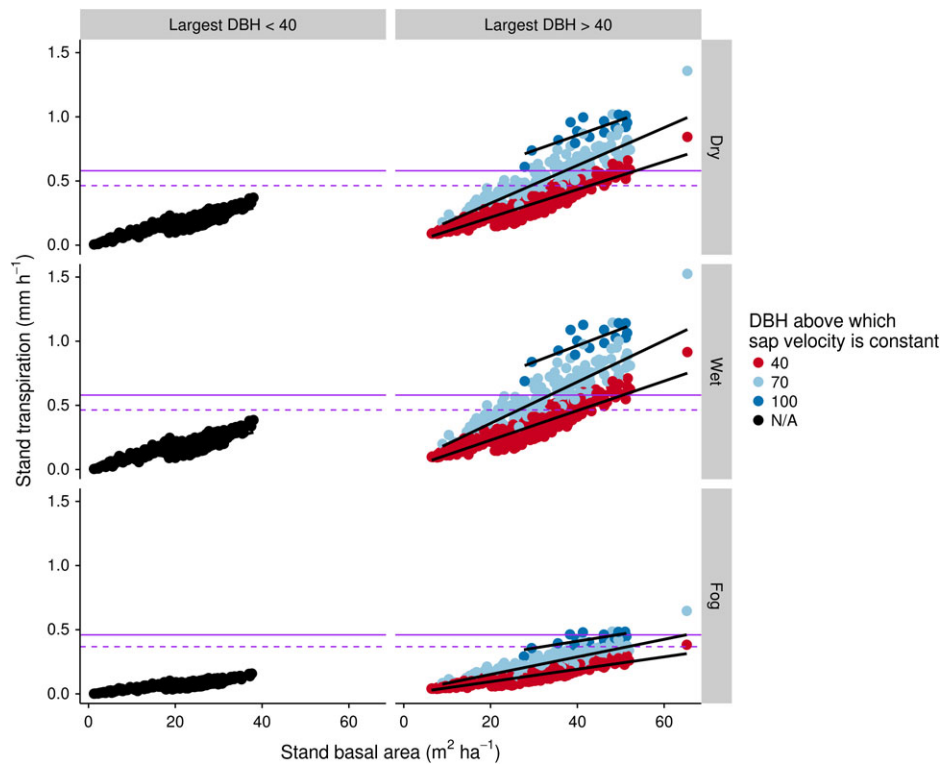


Figure 4. Modeled outputs of stand transpiration against stand basal area across dry, wet and fog seasons. Analyses were separated into plots where the largest trees were less than 40 cm DBH (left) and greater than 40 cm DBH (right). Additionally, the  $V_s$  of large trees were allowed to vary across plots, with asymptotes at 40 cm, 70 cm or 100 cm DBH to simulate a reduction in water use in large trees. Purple lines represent the corresponding net radiation and the dotted lines represent 80% of those values.

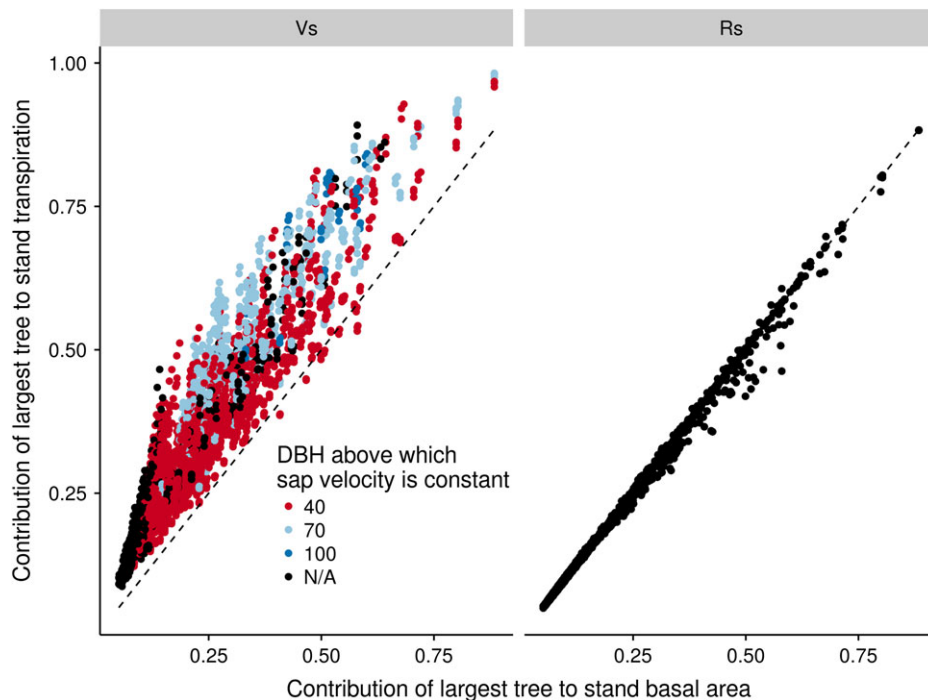


Figure 5. Modeled output of the contribution of the largest tree to stand transpiration against its contribution to stand basal area. In the left panel  $V_s$  is allowed to vary based on the point in the tree when sap velocity is held constant. The right panel holds  $V_s$  constant and allows  $R_s$  to vary as a function of the absolute sapwood depth or as a proportion of the radius.

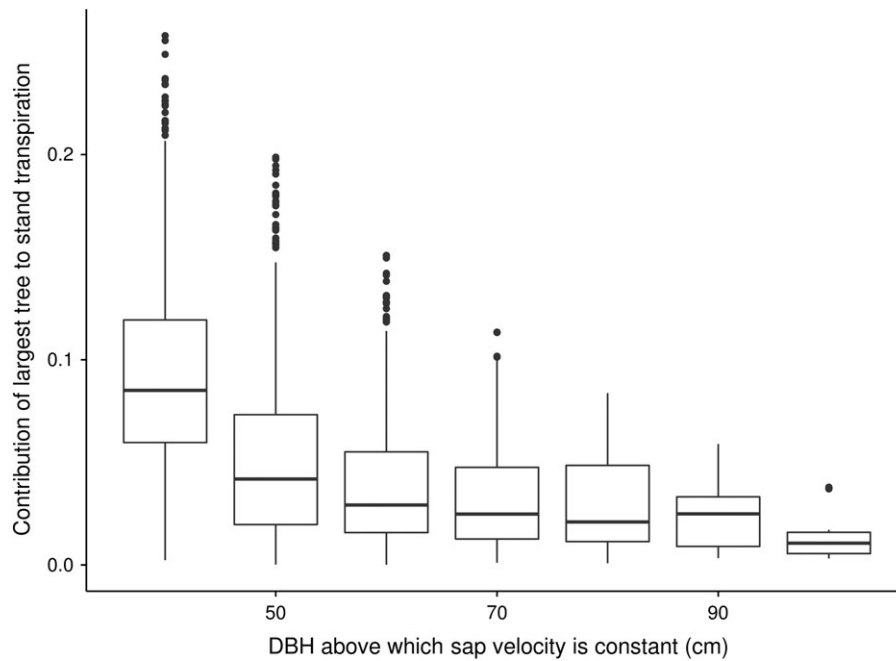


Figure 6. The difference between estimates of transpiration by the DBH at which  $V_s$  and  $R_s$  are held constant. Note that there are large differences in estimates if these values are held constant at smaller trees than larger trees. In each box plot, the midline represents the median, the box represents the first and third quartiles (25th and 75th percentiles), the whiskers represents all values within 1.5 times the interquartile range, and all individual points are values outside 1.5 times the interquartile range.

theoretical maximum was reached at progressively larger stand basal areas (Figure 4). This provides support that actual tree water use in the largest trees is likely less than expected from a linear relationship. Generally this signifies a tendency to overestimate stand transpiration for more dense plots or plots with very large trees based on current sap flow scaling methodologies.

Several prior studies have examined the relationships of sap velocity ( $V_s$ ) and sapwood depth ( $R_s$ ) with respect to tree size. Notably, McIlannet et al. (2007) and Jung et al. (2011) found similar positive linear relationships between  $V_s$  and DBH; however, these relationships were weak. Similar linear relationships have been found between DBH and  $R_s$  (e.g., Wullschlegel and King 2000, Kume et al. 2009, Jung et al. 2011, Looker et al. 2016). Although several studies have highlighted linear relationships between these parameters, this study considered alternative scaling relationships in large trees for two reasons: (i) it is likely that beyond a particular tree size there is a 'diminishing return' of water transport (Meinzer et al. 2001, 2005, Manzoni et al. 2013); and (ii) the difficulty and improbability of sampling the largest trees within the landscape necessitates extrapolation of these relationships. For example, Meinzer et al. (2005) provides strong support for asymptotic relationships in tree sap flow with diameter and aboveground biomass, particularly for angiosperms. Biologically, this is further supported by evidence that stomatal conductance strongly limits transpiration above a certain size and that tree hydraulic conductivity measurements diminish in larger trees (Mencuccini 2002, Niinemets 2002, Jaskierniak et al. 2016). Our data support the idea that there is likely a maximum value of  $Q$  at a

given DBH evidenced by our comparison with the derived net radiation values. This is complementary to studies that suggest supply side constraints to water transport such as soil water capacity, resistances along the hydraulic pathway, and stomatal and boundary layer resistances at the interface with the atmosphere (e.g., Meinzer et al. 2005, Manzoni et al. 2013).

Ultimately, this manuscript provides new insights for both plant biologists and landscape hydrologists. There is a fundamental need to expand scaling practices and methodologies to address maximum water transport by the largest trees. To date, sap flow estimations of whole-tree water use in large trees typically involves sampling only the outer few centimeters of sapwood area or destructive sampling of large trees and derivation through laboratory methods (e.g., Vertessy et al. 1997). In recent literature, many excellent studies have examined radial variation in sap flow rates, which will undoubtedly improve estimates of tree and stand transpiration (Wullschlegel and King 2000, Gebauer et al. 2008, Alvarado-Barrientos et al. 2013, Berdanier et al. 2016). While some studies have emphasized the importance of characterizing sapwood area (e.g., Ford et al. 2007), assessing variation in sap velocities, particularly in the largest trees, is critical for improving accuracy of  $E_t$  estimates. Further, if scaling is done with respect to sap flow parameters ( $V_s$ ,  $R_s$  or  $P_s$ ) instead of  $Q$ , researchers can better assess the propagated errors associated with extrapolation to unsampled trees (Oren et al. 1998). Future research should focus on integrating models of radial variation, plant hydraulics and wood anatomy to tease apart the mechanistic drivers for sap flow rates. Consequently, when scaling sap flow

measurements, researchers should consider the size distributions within plots carefully and make their best attempts to design sampling strategies to account for this potential variation and ensure adequate representation of larger trees.

In conclusion, we have utilized a rigorous combination of field and model simulations to examine how tree water use scales with size in tropical montane forests. Our modeled output takes into consideration asymptotic relationships between DBH and  $V_s$  as an alternative relationship to a constant linear increase. Using a wide range of parameters we found that stand  $E_t$  values often surpassed the net radiation at median stand basal areas, meaning that they were likely overestimated. This is driven by the large uncertainty in predicting water use in the largest trees throughout the landscape. We propose that this modeling framework is a useful tool for predicting transpiration across landscapes because it considers fundamental biological relationships and a wide range of parameters to produce consistent results of transpiration across stands with different basal areas. Additionally, based on these outputs, it is plausible that the true relationship between sap flow parameters and tree diameter is asymptotic or sigmoidal, but more detailed studies considering the tapering effect of these parameters on plant water use are urgently needed to further elucidate these scaling relationships.

## Supplementary Data

Supplementary Data for this article are available at *Tree Physiology* Online.

## Acknowledgments

Significant field assistance was provided by Víctor Castelazo, Alejandra Cuervo, Mariana Quetzalli, Valerie Tchang and Q'enty Delgado. Sensor construction occurred primarily in the Asbjornsen lab at the University of New Hampshire and the Holwerda Lab at UNAM.

## Conflict of interest

None declared.

## Funding

The authors would like to gratefully acknowledge support from the National Science Foundation (NSF-ICER 1313804), Consejo Nacional de Ciencia y Tecnología (CONACYT) (187,646) and UNAM Programa de Apoyo a Proyectos de Investigación e Innovación Tecnológica (IB100113).

## References

- Alvarado-Barrientos MS, Hernández-Santana V, Asbjornsen H (2013) Variability of the radial profile of sap velocity in *Pinus patula* from contrasting stands within the seasonal cloud forest zone of Veracruz, Mexico. *Agric For Meteorol* 168:108–119.
- Alvarado-Barrientos MS, Holwerda F, Asbjornsen H, Dawson TE, Bruijnzeel LA (2014a) Suppression of transpiration due to cloud immersion in a seasonally dry Mexican weeping pine plantation. *Agric For Meteorol* 186:12–25.
- Alvarado-Barrientos MS, Holwerda F, Geissert DR, Muñoz-Villers LE, Gotsch SG, Asbjornsen H, Dawson TE (2014b) Nighttime transpiration in a seasonally dry tropical montane cloud forest. *Trees* 29:259–274.
- Ambrose AR, Sillett SC, Koch GW, Van Pelt R, Antoine ME, Dawson TE (2010) Effects of height on treetop transpiration and stomatal conductance in coast redwood (*Sequoia sempervirens*). *Tree Physiol* 30:1260–1272.
- Arneth A, Kelliher FM, Bauer G et al. (1996) Environmental regulation of xylem sap flow and total conductance of ariz gmelinii trees in eastern Siberia. *Tree Physiol* 16:247–255.
- Asbjornsen H, Goldsmith GR, Alvarado-Barrientos MS et al. (2011) Ecohydrological advances and applications in plant–water relations research: a review. *J Plant Ecol* 4:3–22.
- Aucoin F (2015) Fadist: Distributions that are sometimes used in hydrology. R package version 2.2. <https://CRAN.R-project.org/package=Fadist>.
- Bailey RL, Dell R (1973) Quantifying diameter distributions with the Weibull Function. *Forest Sci* 19:97–104.
- Barbour MM, Whitehead D (2003) A demonstration of the theoretical prediction that sap velocity is related to wood density in the conifer *Dacrydium cupressinum*. *New Phytol* 158:477–488.
- Benyon RG, Lane PNJ, Jaskierniak D, Kuczera G, Haydon SR (2015) Use of a forest sapwood area index to explain long-term variability in mean annual evapotranspiration and streamflow in moist eucalypt forests. *Water Resour Res* 51:5318–5331.
- Berdanier AB, Miniati CF, Clark JS (2016) Predictive models for radial sap flux variation in coniferous, diffuse-porous and ring-porous temperate trees. *Tree Physiol* 36:932–941.
- Berry ZC, Gotsch SG, Holwerda F, Muñoz-Villers LE, Asbjornsen H (2016) Slope position influences vegetation-atmosphere interactions in a tropical montane cloud forest. *Agric For Meteorol* 221:207–218.
- Burgess SSO, Adams M, Turner NC, Beverly CR, Ong CK, Khan AAH, Bleby TM (2001) An improved heat pulse method to measure low and reverse rates of sap flow in woody plants. *Tree Physiol* 21:589–598.
- Campos A (2008) Evaluación de la calidad del suelo. Instituto de Ecología, A.C. – CONACYT, Xalapa, Ver., México.
- Čermák J, Kučera J, Nadezhdina N (2004) Sap flow measurements with some thermodynamic methods, flow integration within trees and scaling up from sample trees to entire forest stands. *Trees* 18:529–546.
- Cohen Y, Fuchs M, Green G (1981) Improvement of the heat pulse method for determining sap flow in trees. *Plant Cell Environ* 4:391–397.
- Cristiano PM, Campanello PI, Bucci SJ et al. (2015) Evapotranspiration of subtropical forests and tree plantations: a comparative analysis at different temporal and spatial scales. *Agric For Meteorol* 203:96–106.
- Enquist BJ, Brown JH, West GB (1998) Allometric scaling of plant energetics and population density. *Nature* 395:163–165.
- Fernández ME, Gyenge J (2009) Testing Binkley's hypothesis about the interaction of individual tree water use efficiency and growth efficiency with dominance patterns in open and close canopy stands. *For Ecol Manage* 257:1859–1865.
- Ford CR, McGuire MA, Mitchell RJ, Teskey RO (2004) Assessing variation in the radial profile of sap flux density in *Pinus* species and its effect on daily water use. *Tree Physiol* 24:241–249.
- Ford CR, Hubbard RM, Kloeppel BD, Vose JM (2007) A comparison of sap flux-based evapotranspiration estimates with catchment-scale water balance. *Agric For Meteorol* 145:176–185.
- García E (1988) Modificaciones al Sistema de Clasificación Climática de Köppen. Offset Larios, Mexico City, D.F., Mexico.
- Gebauer T, Horna V, Leuschner C (2008) Variability in radial sap flux density patterns and sapwood area among seven co-occurring temperate broad-leaved tree species. *Tree Physiol* 28:1821–1830.

- Gotsch SG, Asbjornsen H, Holwerda F, Goldsmith GR, Weintraub AE, Dawson TE (2014) Foggy days and dry nights determine crown-level water balance in a seasonal tropical montane cloud forest. *Plant Cell Environ* 37:261–272.
- Granier A (1987) Evaluation of transpiration in a Douglas-fir stand by means of sap flow measurements. *Tree Physiol* 3:309–320.
- Hernandez-Santana V, Hernandez-Hernandez A, Vadeboncoeur MA, Asbjornsen H (2015) Scaling from single-point sap velocity measurements to stand transpiration in a multi-species deciduous forest: uncertainty sources, stand structure effects, and future scenario impacts. *Can J For Res* 45:1489–1497.
- Holwerda F, Alvarado-Barrientos MS, González-Martínez TM (2016) Surface energy exchange in a tropical montane cloud forest environment: flux partitioning, and seasonal and land cover-related variations. *Agric For Meteorol* 228–229:13–28.
- Huber B (1932) Beobachtung und Messung pflanzlicher Saftströme. *Ber Dtsch Bot Ges* 50:89–109.
- Jarvis PG (1976) The interpretation of the variations in leaf water potential and stomatal conductance found in canopies in the field. *Philos Trans R Soc B* 273:593–610.
- Jaskierniak D, Kucera G, Benyon R, Lucieer A (2016) Estimating tree and stand sapwood area in spatially heterogeneous southeastern Australian forests. *J Plant Ecol* 9:272–284.
- Jiménez MS, Cermák J, Kucera J, Morales D (1996) Laurel forests in Tenerife, Canary Islands: the annual course of sap flow in *Laurus* trees and stand. *J Hydrol* 183:307–321.
- Jung EY, Otieno D, Lee B, Lim JH, Kang SK, Schmidt MWT, Tenhunen J (2011) Up-scaling to stand transpiration of an Asian temperate mixed-deciduous forest from single tree sapflow measurements. *Plant Ecol* 212:383–395.
- Kallarackal J, Otieno DO, Reineking B, Jung E-Y, Schmidt MWT, Granier A, Tenhunen JD (2013) Functional convergence in water use of trees from different geographical regions: a meta-analysis. *Trees* 27: 787–799.
- Kluitenberg GJ, Ham JM (2004) Improved theory for calculating sap flow with the heat pulse method. *Agric For Meteorol* 126:169–173.
- Koenker R (2016) quantreg: Quantile Regression. R package version 5.29. <https://CRAN.R-project.org/package=quantreg>.
- Köstner B, Granier A, Cermák J (1998) Sapflow measurements in forest stands: methods and uncertainties. *Ann Sci For* 55:13–27.
- Köstner B, Falge E, Tenhunen JD (2002) Age-related effects on leaf area/sapwood area relationships, canopy transpiration and carbon gain of Norway spruce stands (*Picea abies*) in the Fichtelgebirge, Germany. *Tree Physiol* 22:567–574.
- Köstner BMM, Schulze E-D, Kelliher FM, Hollinger DY, Byers JN, Hunt JE, McSeveny TM, Meserth R, Weir PL (1992) Transpiration and canopy conductance in a pristine broad-leaved forest of *Nothofagus*: an analysis of xylem sap flow and eddy correlation measurements. *Oecologia* 91:350–359.
- Kume T, Tsuruta K, Komatso H, Kumagai T, Higashi N, Shinohara Y, Otsuki K (2009) Effects of sample size on sap flux-based stand-scale transpiration estimates. *Tree Physiol* 30:129–138.
- Link P, Simonin K, Maness H, Oshun J, Dawson TE, Fung I (2014) Species differences in the seasonality of evergreen tree transpiration in a Mediterranean climate: analysis of multiyear, half-hourly sap flow observations. *Water Resour Res* 50:1869–1894.
- Looker N, Martin J, Jencso K, Hu J (2016) Contribution of sapwood traits to uncertainty in conifer sap flow as estimated with the heat-ratio method. *Agric For Meteorol* 223:60–71.
- Loustau D, Berbigier P, Roumagnac P, Arruda-Pacheco C, David JSS, Ferreira MI, Pereira JS, Tavares R (1996) Transpiration of a 64-year-old maritime pine stand in Portugal. 1. Seasonal course of water flux through maritime pine. *Oecologia* 107:33–42.
- Manzoni S, Vico G, Katul G, Palmroth S, Jackson RB, Porporato A (2013) Hydraulic limits on maximum plant transpiration and the emergence of the safety–efficiency trade-off. *New Phytol* 198:169–178.
- Marshall DC (1958) Measurement of sap flow in conifers by heat transport. *Plant Physiol* 33:385–396.
- Martin TA, Brown KJ, Kucera J, Meinzer FC, Sprugel DG, Hinkley TM (2000) Control of transpiration in a 220-year-old *Abies amabilis* forest. *For Ecol Manage* 152:211–224.
- McLannet D, Fitch P, Disher M, Wallace J (2007) Measurements of transpiration in four tropical rainforest types of north Queensland, Australia. *Hydrol Proc* 21:3549–3564.
- Meinzer FC, Goldstein G, Andrade JL (2001) Regulation of water flux through tropical forest canopy trees: do universal rules apply? *Tree Physiol* 21:19–26.
- Meinzer FC, Bond BJ, Warren JM, Woodruff DR (2005) Does water transport scale universally with tree size. *Func Ecol* 19:558–565.
- Meir P, Grace J (2002) Scaling relationships for woody tissue respiration in two tropical rain forests. *Plant Cell Environ* 25:963–973.
- Mencuccini M (2002) Hydraulic constraints in the functional scaling of trees. *Tree Physiol* 22:553–565.
- Mitchell PJ, Lane PN, Benyon RG (2012) Capturing within catchment variation in evapotranspiration from montane forests using LiDAR canopy profiles with measured and modelled fluxes of water. *Ecohydrology* 5:708–720.
- Muñoz-Villiers LE, López-Blanco J (2008) Land use/cover changes using Landsat TM/ETM images in a tropical and biodiverse mountainous area of central-eastern Mexico. *Int J Remote Sens* 29:71–93.
- Muñoz-Villiers LE, Holwerda F, Gómez-Cárdenas M, Equihua M, Asbjornsen H, Bruijnzeel LA, Marín-Castro BE, Tobón C (2012) Water balances of old-growth and regenerating montane cloud forests in central Veracruz, Mexico. *J Hydrol* 462–463:53–66.
- Novick K, Oren R, Stoy P, Juang JY, Siqueira M, Katul G (2009) The relationship between reference canopy conductance and simplified hydraulic architecture. *Adv Water Res* 32:809–819.
- Niinemets Ü (2002) Stomatal conductance alone does not explain the decline in foliar photosynthetic rates with increasing tree age and size in *Picea abies* and *Pinus sylvestris*. *Tree Physiol* 22:515–535.
- Oren R, Phillips N, Katul G, Ewers BE, Pataki DE (1998) Scaling xylem sap flux and soil water balance and calculating variance: A method for partitioning water flux in forests. *Ann Sci For* 55:191–216.
- Oren R, Phillips N, Ewers BE, Pataki DE, Magonigal JP (1999) Sap-flux-scaled transpiration responses to light, vapor pressure deficit, and leaf area reduction in a flooded *Taxodium distichum* forest. *Tree Physiol* 19: 337–347.
- R Development Core Team (2016) R Development Core Team R: A Language and Environment for Statistical Computing R Foundation for Statistical Computing. Vienna, Austria (<http://www.R-project.org>)
- Ryan MG, Yoder BJ (1997) Hydraulic limits to tree height and tree growth. *BioScience* 47:235–242.
- Schäfer KVR, Oren R, Tenhunen JD (2000) The effect of tree height on crown level stomatal conductance. *Plant Cell Environ* 23:365–375.
- Smith DD, Sperry JS, Enquist BJ, Savage VM, McCulloh KA, Bentley LP (2014) Deviation from symmetrically self-similar branching in trees predicts altered hydraulics, mechanics, light interception and metabolic scaling. *New Phytol* 201:217–229.
- Sperry JS, Smith DD, Savage VM, Enquist BJ, McCulloh KA, Reich PB, Bentley LP, von Allmen EI (2012) A species-level model for metabolic scaling in trees I. Exploring boundaries to scaling space within and across species. *Funct Ecol* 26:1054–1065.
- Vertessy R, Hutton TJ, Reece P, O'Sullivan SK, Benyon RG (1997) Estimating stand water use of large mountain ash trees and validation of the sap flow measurement technique. *Tree Physiol* 17:747–756.
- West GB, Brown JH, Enquist BJ (1997) A general model for the origin of allometric scaling laws in biology. *Science* 276:122–126.



- Williams-Linera G (2002) Tree species richness complementarity, disturbance and fragmentation in a Mexican tropical montane cloud forest. *Biodiv Conserv* 10:1825–1843.
- Williams-Linera G, Manson RH, Isunza-Vera E (2002) La fragmentación del bosque mesófilo de montaña y patrones de uso del suelo en la región oeste de Xalapa, Veracruz, México. *Madera Bosques* 8:73–89.
- Williams-Linera G, Toledo-Garibaldi M, Hernández CG (2013) How heterogeneous are the cloud forest communities in the mountains of central Veracruz, Mexico? *Plant Ecol* 214:685–701.
- Wilson KB, Hanson PJ, Mulholland PJ, Baldocchi DD, Wullschleger SD (2001) A comparison of methods for determining forest evapotranspiration and its components: sap-flow, soil water budget, eddy covariance and catchment water balance. *Agric For Meteorol* 106:153–168.
- Wullschleger SD, King AW (2000) Radial variation in sap velocity as a function of stem diameter and sapwood thickness in yellow-poplar trees. *Tree Physiol* 20:511–518.
- Wullschleger SD, Meinzer FC, Vertessy RA (1998) A review of whole-plant water use studies in trees. *Tree Physiol* 18:499–512.
- Yoder BJ, Ryan MG, Waring RH, Schoettle AW, Kaufmann MR (1994) Evidence of reduced photosynthetic rates in old trees. *Forest Sci* 40:513–527.
- Zeide B (1995) A relationship between size of trees and their number. *For Ecol Manage* 72:265–272.
- Zimmermann R, Schulze ED, Wirth C, Schulze EE, McDonald KC, Vygodskaya NN, Ziegler W (2000) Canopy transpiration in a chronosequence of Central Siberian pine forests. *Glob Chang Biol* 6:25–37.